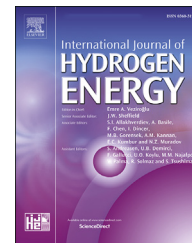




ELSEVIER

Available online at www.sciencedirect.com

ScienceDirect

journal homepage: www.elsevier.com/locate/he

Investigation of hydrogen usage on combustion characteristics and emissions of a spark ignition engine

Yasin Karagöz ^{a,*}, Özgün Balcı ^a, Hasan Köten ^b^a Automotive Division, Department of Mechanical Engineering, Mechanical Engineering Faculty, Yildiz Technical University, Yildiz, Besiktas, Istanbul, 34349, Turkey^b Department of Mechanical Engineering, Engineering Faculty, University of Medeniyet, Kadıköy, Istanbul, 34000, Turkey

ARTICLE INFO

Article history:

Received 31 August 2018

Received in revised form

9 January 2019

Accepted 14 January 2019

Available online xxx

Keywords:

Hydrogen

NO_x

THC

CO

Heat release rate

ABSTRACT

In this study, initially, a single cylinder, naturally aspirated, spark ignition engine was loaded with AC engine dynamometer and a spark plug type engine transducer was used to obtain in-cylinder pressure. The test engine was operated with gasoline fuel at full load and different engine speeds (3100, 3200, 3300, 3400 and 3450 rpm). Secondly, using obtained engine performance, emission values and in-cylinder pressure, a one dimensional engine model was built and validated by an engine performance and emission analysis software (AVL-Boost). After the validation of single dimensional theoretical engine model, a comparison was made between the emission, performance and combustion (in-cylinder pressure, rate of heat release) values of operations with pure hydrogen fuel and such values of the operations with unleaded gasoline. The emissions of CO and total hydrocarbons (THC) were negligible with using hydrogen as fuel in SI engine. A dramatic increase in NO_x emissions was obtained with using hydrogen as fuel. However, by using hydrogen in lean conditions, NO_x emissions were taken under control by means of wide flammability limits of hydrogen.

© 2019 Hydrogen Energy Publications LLC. Published by Elsevier Ltd. All rights reserved.

Introduction

Rising air pollution caused by energy sources has led to a need for cleaner energy sources. Fossil fuels meet a large part of energy needs at the present time. According to the EPA, the transportation sector was responsible for approximately 23% of total energy-related CO₂ emissions in 2010 [2014, [1]].

Many methods such as fuel cell (FC), proton exchange membrane fuel cells (PEMFC), electric and hybrid vehicles as

well as partly or fully hydrogen-fueled ICEs have been developed in order to replace some of the energy needs of petroleum fuels. Among these methods, it takes time for electric vehicles to become broad due to the lack of battery technology and widespread use of charging stations [2016, [2]]. Fuel-cell and PEMFC technologies, however, remain very limited due to the difficulty of purifying hydrogen, their high cost and service life [2014, [1]]. The use of ICEs is more advantageous than conventional engines in terms of thermal efficiency and especially CO and THC emissions.

* Corresponding author.

E-mail address: ykaragoz@yildiz.edu.tr (Y. Karagöz).

<https://doi.org/10.1016/j.ijhydene.2019.01.147>

0360-3199/© 2019 Hydrogen Energy Publications LLC. Published by Elsevier Ltd. All rights reserved.

Some researchers [2018, [3]], [2018, [4]] have investigated alternative fuels such as ethanol, biodiesel, CNG, etc. Among these fuels, hydrogen is the most important alternative fuel thanks to its physico-chemical properties. Hydrogen has its own properties, such as a very high diffusion coefficient and flame speed [2009, [5]]. Because of these features, when used as an additional fuel or pure, the combustion process approaches the ideal constant volume cycle thus increasing thermal efficiency [2009, [6]]. In addition, due to the wide flammability-limits feature of hydrogen, SI engines can operate in extremely lean conditions.

Some previous studies on the use of hydrogen fuel at lean conditions are presented below.

Heffel [2003, [7]] experimentally investigated the effects of EGR and TWC on NO_x and the performance in a 4-cylinder hydrogen fueled SI engine at 3000 rpm engine speed in terms of equivalence ratio, hydrogen and EGR. Experiments were performed between lean burn and stoichiometry conditions. As a result of these experiments, the maximum torque was obtained (94 Nm, 88 Nm respectively) with lean-burn strategy compared to the EGR when the engine was based on the knocking limit. While based on NO_x emission condition of about zero, more torque was obtained (88 Nm, 55 Nm respectively) than the lean-burn strategy with EGR.

Dhyani and Subramanian [2018, [8]] studied the effects of knocking parameters such as spark timing, injection timing, and equivalence ratio on the multi-cylinder hydrogen fueled SI engine at 1500 rpm engine speed. As a result of the study, it was observed that knock and backfire were related to each other at high equivalence ratio and that spark and injection timing of 12° BTDC, 40° ATDC respectively inhibited backfire.

Li and Karim [2004, [9]] studied the equivalence ratio regions in which the hydrogen filled SI engine can operate without knock, depending on the compression ratio, intake temperature and spark timing in both modelled and experimental runs. It is seen that compression ratio and intake temperature have a much greater effect on knock formation than spark timing.

Verhelst et al., [2009, [10]] conducted an experimental study on a bi-fuel hydrogen/gasoline engine, in which they can alter the start of combustion, injection duration and intake valve timings. They firstly, determined equivalence ratio threshold for NO_x formation at WOT, hydrogen operation. Then different hydrogen gasoline operations were compared and analyzed. As result, they observed that hydrogen operations were more advantageous than gasoline operations at all speeds and than the loads combinations (especially at low loads) in terms of brake thermal efficiency, despite the thermal efficiency reduction of hydrogen operations at higher loads caused by NO_x emissions control.

Some previous studies on the use of hydrogen fuel are given below.

Different EGR rates (12–47% by mass) at stoichiometric condition was used in the experimental and numerical investigation of Kosmadakis et al., [2012, [11]] in order to decrease NO_x emissions and control load of hydrogen fueled SI engine. CFD code, which includes laminar flame speed formula that has residual gas term, was also built and validated. The results showed that the combustion durations varied between 10°–80° CA by increasing EGR rate. They

concluded that EGR application is more effective on reduction of NO_x emissions than hydrogen lean operation engine load control.

Nieminen and Dincer [2010, [12]] conducted a model exergy study to compare gasoline and hydrogen fuels at the SI engine. As a result, they observed that hydrogens chemical exergy turned into more useful work and thus increased second law efficiency.

Lucas and Richards [1982, [13]] used hydrogen as pure fuel in idle operation and as supplementary fuel in partial loads in their research. Under these conditions, the efficiency increased by 10% and the CO and NO_x emissions decreased by 28.3% and 9.8%, respectively.

Ji et al., [2013, [14]] investigated the effects of only hydrogen and hydrogen addition to SI engine fueled by gasoline during a cold start. They carried out the tests according to New European Driving Cycle under stoichiometric condition. Hydrogen was provided by onboard water electrolysis generator during the experiments. For the first test, the vehicle was operated with hydrogen fuel for the first 7 s, and then, hydrogen was gradually reduced down to zero while simultaneously, gasoline fraction was being gradually increased up to 100% in the following 4 s. For the second test process, hydrogen fraction was kept at 3% by volume after the same transient process with that of the first test (after 11 s) in order to compare pure gasoline operation of the first test and hydrogen addition after cold start. The process can be summarised as below:

- First test: I) 100% hydrogen and zero gasoline operation (first 7 s), II) gradually reduction of hydrogen down to zero and gradual increase of gasoline up to 100% operation (following 4 s) III) 100% gasoline and zero hydrogen operation (rest of the test).
- First test: I) 100% hydrogen and zero gasoline operation (first 7 s), II) gradual reduction of hydrogen down to 3% and gradual increase of gasoline up to 97% operation (following 4 s) III) 97% gasoline and 3% hydrogen operation (rest of the test).

According to test results, these two procedure provided reduction in CO and HC emissions but the first procedure improved CO and HC values by 62.1% (from 1.61 g/100 km to 0.61 g/100 km) and 64.1% (from 0.22 g/100 km to 0.079 g/100 km) in comparison to only gasoline operation, respectively.

Some researchers have studied the effect of natural gas or methane–hydrogen blends as fuel on combustion, flame velocities, performance and emissions. Some of these studies are presented below.

Huang et al., [2006, [15]] experimentally investigated laminar flame characteristics of different fractions of natural gas–hydrogen–air blends at different equivalence ratios (varied 0–100% and 0.6–1.4, respectively) in terms of burning velocity, flame expansion, flame radius and flame stretch rate. The experiments were conducted by using a constant volume bomb, which includes pressure sensor, thermocouple and electrodes. Their results showed a linear correlation between flame radius-time for blends that have high hydrogen fractions and a stoichiometric equivalence ratio. A decreasing rate of increase in the flame radius versus time was obtained for

blends which have a low equivalence ratio and low hydrogen fractions. Conversely, there is an increasing rate of increase in the flame radius versus time for blends that have a high equivalence ratio and low hydrogen fractions. Additionally, an empirical formula of flame speed was proposed by using experimental data.

Hu et al., [2009, [16]] conducted another study about flame characteristics of natural gas–hydrogen–air blends experimentally and numerically. In this study, the researchers conducted their investigations with a broader range of equivalence ratio for rich mixtures. Digital flame photographs were also used in order to observe flame radius in time. As their conclusion, laminar burning velocities were analyzed in three different regimes depending on hydrogen methane fractions. They obtained similar results in addition to a strong relationship observed between the H and OH radicals' concentration and burning velocity.

Huang et al., [2007, [17]] experimentally investigated natural gas–hydrogen blends in an SI engine in terms of combustion and HRR values. Their results showed that with a constant excess air ratio and spark timing, which provides the maximum engine torque, rich mixtures have higher peak-pressure and HRR values with natural gas while 10% hydrogen fraction provides the maximum peaks with stoichiometric and lean mixtures.

A similar experimental investigation was conducted by Huang et al., [2006, [18]]; however, in this study, the researchers conducted their study with both performance and emission data of natural gas–hydrogen blends combustion. They found that for a constant excess air ratio and increasing hydrogen content, decreasing and increasing thermal efficiency trends were obtained before and after a 20% hydrogen fraction, respectively. Moreover, by increasing the hydrogen content, HC emissions were decreasing while NO_x emissions were increasing.

Hu et al., [2009, [19]] experimentally investigated the effects of EGR rates on performance and emissions with natural gas–hydrogen-fueled SI engines. They found that an increase of hydrogen content in fuel can compensate for an engine output reduction caused by high rates of EGR operation.

Hu et al., [2009, [20]] investigated the effects of EGR and hydrogen content in hydrogen–natural gas blends in terms of combustion characteristics. They found that larger EGR operations cause an increase in flame development, rapid combustion and total combustion durations, while a higher hydrogen content provides reduction. Moreover, a higher hydrogen content in fuel becomes more important at a larger EGR operation in order to decrease COV_{BMEP}.

Some previous studies on the use of hydrogen as an additional fuel are provided below.

Ceviz et al., [2012, [21]] studied hydrogen addition to gasoline with a spark-ignition engine. They carried out their experiments at 2000 rpm constant engine speed and by using 0%, 2.14%, 5.28% and 7.74% hydrogen fractions by volume as fuel. The test results showed that the addition of hydrogen provided improvement in the total brake-specific fuel consumption, HC and CO emissions due to higher flame speed and to being a fuel without C atoms, while the NO_x emissions were increased.

As mentioned above and seen in the study results, the use of hydrogen as an additional fuel can improve the thermal efficiency and improve the CO and THC emissions. The thermal efficiency improvement is further improved due to its characteristic properties with the pure use of hydrogen, while CO and THC emissions were almost non-existent. However, under these operating conditions, NO_x emissions were significantly increased due to high temperatures. Utilizing the wide flammability limits of the hydrogen [2008, [22]], an extremely lean air–hydrogen mixture can be burned, and NO_x emissions can be controlled. Currently, a hydrogen-fueled engine which doesn't need a gas throttle is expected to be an efficient option even though the volumetric efficiency is low, considering that the importance of low-power and hybrid-oriented engines as well as hybrid power generation systems increases.

Operation conditions around stoichiometry or richer are more advantageous for SI engines in terms of brake power and the engines' efficiency [2014, [23]]; however, these conditions cause more emissions, especially NO_x formations [2016, [24]], which have significant negative effects on human health.

Studies in the literature have showed that hydrogen addition causes large amount of NO_x emissions increase, especially at full load. On the other hand, it provides decrease in CO, CO₂ and THC emissions thanks to unique properties of hydrogen in addition to being carbon free fuel. However, it is observed that the studies, which are focused on SI engines with extremely lean pure hydrogen operations by benefiting from wide flammability limits of hydrogen, are not sufficient. Therefore, hydrogen fueled SI engine operations are investigated at extremely lean conditions in this study.

Thus, hydrogen use as fuel can be a solution for THC, CO and CO₂ emissions, while a lean hydrogen air mixture helps to keep NO_x formations under control owing to a higher flame speed and broader flammability range of hydrogen fuel. In the literature, the effects of hydrogen addition to an SI or CI engine on performance and emissions and the effects of hydrogen addition on lean burn limit improvement has been extensively investigated. However, studies on the use of hydrogen as fuel and the effects on performance and emission characteristics of hydrogen operating conditions are not sufficient. For this reason, the one-dimensional engine model developed by the light duty SI engine with the experimental results obtained with the petrol working condition was confirmed in this study. After confirming the theoretical model, it was compared to the condition of neat hydrogen operation and the operation condition of neat gasoline fuel. In the last phase of the study, the effect of using hydrogen fuels in SI engines in different air excess coefficients and in lean and extremely lean conditions, especially to control NO_x emissions, has been theoretically investigated. To put it briefly, the main purpose of this study is to build an analyzed and experimentally validated 1-D theoretical model (0-D combustion model), which produces fast and reliable results for a hydrogen-fueled SI engine. Another aim of this study is to determine lean operation parameters in order to suppress a dramatic increase in NO_x caused by hydrogen use by means of wide flammability limits of hydrogen with the help of a built theoretical model.

Materials and test methods

Fig. 1 shows the schematic illustration of the test set up of a single-cylinder SI engine. Single-cylinder, naturally aspirated, four-stroke, SI engines were loaded with an AC dynamometer to perform tests. The rest of the test setup consists of exhaust and emission gas analyses system and data acquisition and post processing system. The properties of the test setup and test devices are described in the following sections.

Experimental setup

Tests were carried out on single cylinder, four stroke and naturally aspirated SI engine. Experiments were carried out under gasoline engine operating conditions. The gasoline flow rate was measured by a miniature oval gear flow meter. In addition, with the gravimetric method, 0.1 gr. the consumption of the fuel in the fuel tank was measured by means of the scale with precision, and the fuel consumption was verified. Introduced intake air measurement was performed with a thermal mass flow meter. An AC dynamometer and resistive load banks were used in order to load SI engine. Emission measurement was performed with an AVL Digas 4000 tailpipe emission analyzer. The AVL Digas 4000 measured CO and THC emissions using the infrared method while NO_x emissions were achieved using the electrochemical method. On the other hand, CO emission values obtained were on volume% basis while NO_x and THC emission values obtained are given in terms of ppm. As the engine power values changed in the experiments due to having operated at different cycles, the

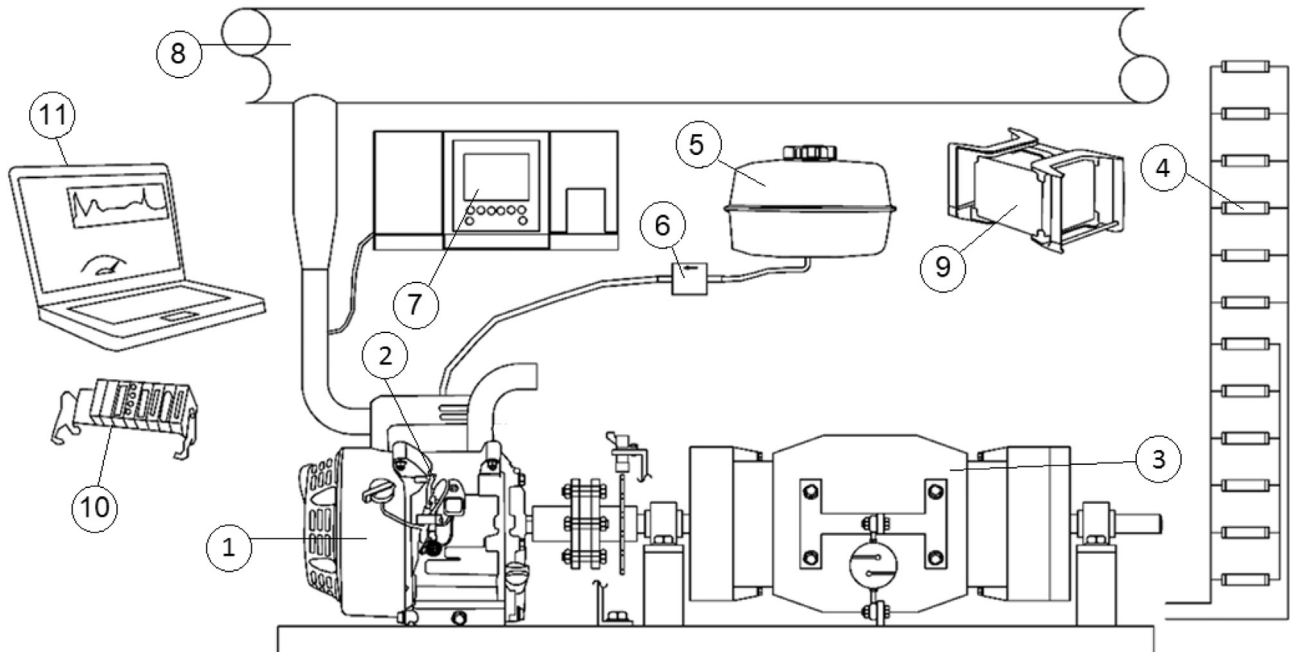
values obtained were converted into specific emission values taking VDMA exhaust emission legislation into consideration. The engine speed was measured by the proximity type sensor. In addition, an incremental type encoder was used to determine the crank angle and piston position. Cylinder pressure data was measured with the aid of the spark plug type cylinder pressure sensor. Also, combustion analysis was performed with a Kistler Kibox combustion analyzer.

Engine specs and dynamometer features

Single-cylinder, 4-stroke, naturally aspirated, light duty type spark ignition engine was used as the test engine. The engine was loaded with an AC dynamometer connected directly to the SI engine. The SI engine and the engine dynamometer specifications are presented below in Table 1. All tests were performed at Internal Combustion Engines Laboratory of Yildiz Technical University.

Modelling of the test engine

In operation, the single-cylinder, four-stroke, naturally aspirated engine was modelled as one-dimensional with the aid of Boost software. The one-dimensional (1-D) model developed with the Boost software of the test engine is given in Fig. 2. The Woschni heat transfer model was used in this study and the same parameters were used for all engine speeds of gasoline operations. However, revised parameters are used for different equivalence ratios of hydrogen operations by taking quenching

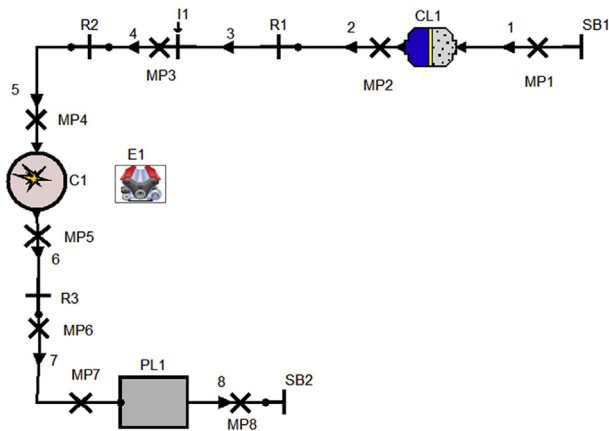


1. Test engine
2. Pressure sensor
3. Dynamometer
4. External resistive load banks
5. Gasoline tank
6. Gasoline flowmeter
7. Exhaust gas analyser
8. Exhaust ventilation system
9. Kibox combustion analyser
10. NI data acquisition device
11. Personal computer for data recording and post processing

Fig. 1 – Schematic diagram of engine test system.

Table 1 – The SI engine and dyno specifications.

Engine specs	
Manufacturer company	Honda
Number of cylinders	1
Compression ratio	8.5:1
Cooling	Air
Bore × stroke [mm]	77 × 58
Cylinder volume [cm ³]	270
Net power [kW]	6.3/3600 rpm
Recommended speed range [rpm]	2000–3500
Aspiration	Natural
Dyno Specs	
Power [kW]	8

**Fig. 2 – One dimensional model of the test engine in Boost software.**

distance into consideration since quenching distance (and hence, thermal boundary) of hydrogen is thinner than that of gasoline. Moreover, the quenching distance of hydrogen increases by increasing the air excess ratio. The Vibe two-zone combustion model used was verified with the help of the experimental data obtained. The start of combustion, combustion duration and shape parameter of the gasoline-fueled model are determined by a normalized heat release rate calculated from pressure data which were obtained by laboratory engine test results. The formulations used to calculate heat release rate values can be seen in the 'Data Reduction' section. For hydrogen-fueled modelling, the start of combustion was delayed by taking the maximum brake mean effective pressure into consideration. Combustion duration and shape parameters were determined based on the previous studies and by using flame speed values of the hydrogen combustion process. The results of theoretical and experimental data obtained using gasoline are given in Table 2. From the obtained results, the maximum error rate was observed in THC emission and found to be 6.02% of the measured value. The comparison of experimentally obtained pressure data and heat-release rates is given in Fig. 3 for engine speed of 3300 rpm. The results show that in-cylinder pressure data and normalized heat-release rate data were superimposed. This seems to be acceptable for the model validation.

In Fig. 3, a proportionally high difference between theoretical and experimental in-cylinder pressure values, which

Table 2 – Comparison and validation of experimental and theoretical emission and performance results.

	Experimental	Simulation	Error %
Max pressure [bar]	29.918	29.041	2.93
Max HRR [-]	0.02682	0.02749	2.49
BTE [%]	23.646	23.99	1.46
CO [g/kWh]	176.39	168.45	4.5
THC [g/kWh]	7.64	7.18	6.02
NO _x [g/kWh]	0.598	0.611	2.17
Ne [kW]	6.15	6.38	3.74

are gathered at intake and the beginning of compression time, is shown. Although the pressure data received at intake and the beginning of compression through the cylinder has very low values, the pressure sensor used in this study is designed to perform high pressure measurements. Moreover, the spark plug-type pressure sensor had to be located vertically due to constructive restrictions such as water channels. Therefore, the error ratio is relatively large in proportion to the pressure values obtained from the simulations, especially at the intake time. This difference is predicted not to cause a fault in the examination of the engine performance, emissions and combustion processes, since it occurs at the time of intake.

Data reduction

The followings are calculation methods used for engine performance, specific emissions and heat release rate values.

Brake engine torque equation can be obtained as shown in Eq. (1) can be calculated by using load cell data.

$$M_e = F.L \quad (1)$$

where, F is force value which was obtained from load cell and L is distance between dynamometer axis and applying force axis through the load cell.

By use of brake engine torque value, brake engine power (N_e) can be calculated as given in Eq. (2) [25].

$$N_e = \frac{2\pi n}{60} M_e \quad (2)$$

where, M_e is brake engine torque (Nm) and n is the engine velocity (rpm).

Brake mean effective pressure (BMEP) (MPa) value can be reached as in Eq. (3).

$$BMEP = M_e \frac{4 \cdot \pi}{V_H} \quad (3)$$

where, V_H is engine swept volume (cm³).

Brake thermal efficiency can be calculated as given in Eq. (4) [26].

$$BTE = \frac{N_e}{\dot{m}_f \times LHV_f} \quad (4)$$

where, BTE is brake thermal efficiency, \dot{m}_f is mass flow rate of gasoline or hydrogen (kg/s) and LHV_f is lower heating values of gasoline or hydrogen (kJ/kg).

Below Eq. (5) is used in order to calculate gasoline equivalent brake specific fuel consumption values [27].

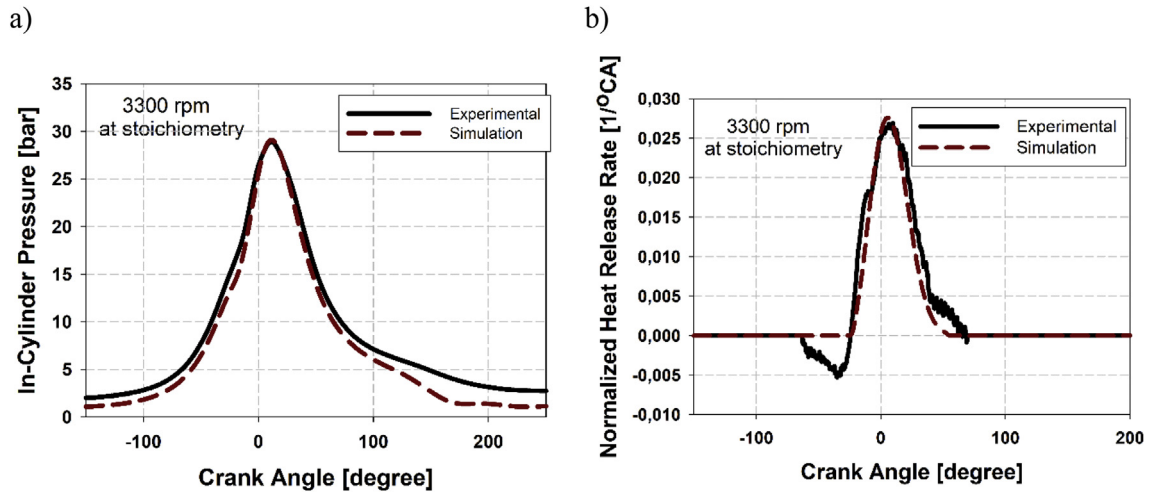


Fig. 3 – a) Comparison and validation of experimental and simulation results of a) in-cylinder pressure and b) normalized heat release rate.

$$BSFC = \frac{\dot{v}_f \cdot \rho_f}{N_e} \frac{3600}{1000} \frac{LHV_f}{LHV_g} \quad (5)$$

where, \dot{v}_f (cm^3) and ρ_f (kg/m^3) are volume flow rate and density of fuel, respectively. LHV_f and LHV_g (MJ/kg) lower heating value of fuel and lower heating value of gasoline, respectively.

Cylinder volume can be calculated as given in Eq. (6) below [28].

$$V = \frac{V_H}{2} \left[(1 - \cos\alpha) + \frac{\phi}{4} (1 - \cos 2\alpha) \right] \frac{LHV_f}{LHV_g} \quad (6)$$

where, α is crank position (rad) and ϕ is crank radius-connecting rod length ratio.

Rate of heat release was obtained as given in Eq. (7) [29].

$$\dot{Q} = \frac{k}{k-1} P \frac{dV}{d\theta} + \frac{k}{k-1} V \frac{dP}{d\theta} \quad (7)$$

where, \dot{Q} is heat release rate (HRR) ($\text{J}/^\circ\text{CA}$) and k is working mixture polytropic index. Also, normalized values were used in the manuscript. This equation was used solely to pass from experimental pressure data to normalized heat release rate values.

Heat release rate values were obtained by using Vibe function as shown in EqS. (8)–(10) [30].

$$\frac{dx}{d\alpha} = \frac{\alpha}{\Delta\alpha_c} (m+1)y^m e^{-a y^{(m+1)}} \quad (8)$$

$$dx = \frac{dQ}{Q} \quad (9)$$

$$y = \frac{\alpha - \alpha_0}{\Delta\alpha_c} \quad (10)$$

where, Q is total fuel heat input, α is crank angle, α_0 is crank angle at the beginning of combustion, $\Delta\alpha_c$ is combustion duration, m is shape parameter, a is Vibe parameter which is equal to 6.9 for complete combustion as a property of Vibe function [30]. The parameters of Vibe function were approximated by also using mass fraction burned equation of Vibe.

Air excess ratio of eventual fuel blend (gasoline or hydrogen) can be calculated by using Eq. (11) written as follows [23].

$$\lambda = \frac{\dot{v}_{air} \rho_{air}}{\dot{v}_f \rho_f AF_{st,f}} \quad (11)$$

where, λ is air excess ratio of fuel blend, \dot{v}_{air} and ρ_{air} are air flow rate and density, respectively, $AF_{st,f}$ and $AF_{st,g}$ is stoichiometric air-to-fuel ratio of fuel (gasoline or hydrogen).

Specific exhaust gas emissions were obtained on volume basis using gas analyzer. Using flow rate of tailpipe gases, the specific exhaust gas emission values can be realized. The tailpipe gas flow rate can be obtained adding intake air and consumed fuel flow rates as given in Eq. (12) [31]. Therefore, specific emissions EP_i (pollutant mass, i , referenced to P_{eff}) can be realized as given in Eq. (13) [31].

$$\dot{m}_{exh} = \dot{m}_{int} + \dot{m}_f \quad (12)$$

$$EP_i = EV_i \frac{M_i}{M_{exh}} \frac{\dot{m}_{exh}}{N_e} \quad (13)$$

where, \dot{m}_{exh} and \dot{m}_{int} is mass flow rates of exhaust gases and intake air (g/h), EP_i is specific emission value (pollutant mass, i , referenced to P_{eff}) of gases (g/kWh), EV_i is relevant gases quantity (exhaust emission value of components, i , as volume share (ppm or %)) in proportion to total exhaust gases and M_i and M_{exh} are molar mass of relevant gases and exhaust gases (kg/kmol), respectively.

Kline and McClintock analysis [32] was used to calculate total uncertainty W_R as in EqS. (14) And (15).

$$(W_R)_{P, B} = \left[\left(\frac{\partial R}{\partial x_1} w_1 \right)^2 + \left(\frac{\partial R}{\partial x_2} w_2 \right)^2 + \dots + \left(\frac{\partial R}{\partial x_n} w_n \right)^2 \right]^{1/2} \quad (14)$$

where, $(W_R)_{P, B}$ is the propagated uncertainty, x_1, x_2, \dots, x_n are the measured variables and w_1, w_2, \dots, w_n are the uncertainty values of the variables.

Therefore, the total uncertainty W_R is calculated with Eq. (15):

$$W_R = \sqrt{(W_R)_P^2 + (W_R)_B^2} \quad (15)$$

where, $(W_R)_P$ is precision error function and $(W_R)_B$ is systematic (Bias) error function.

Investigation procedure

In the research carried out, engine tests were firstly carried out with 4-stroke, single-cylinder, naturally aspirated SI engine at different engine speeds (3100 rpm, 3200 rpm, 3300 rpm, 3400 rpm and 3450 rpm), full load and stoichiometry by neat gasoline fuel. All tests were performed at Internal Combustion Engines Laboratory of Yildiz Technical University. Then, the one-dimensional (1-D) mathematical model was developed by using AVL Boost software and verified with the experimental in-cylinder pressure, normalized heat release rate, brake thermal efficiency, brake engine power, CO, THC and NO_x data. The validated mathematical model was used to obtain stoichiometric and lean conditions of hydrogen operations results. In order to provide maximum brake mean effective pressure and considering higher flame speed of hydrogen fuel, ignition timing was delayed 3.5° CA during hydrogen operation. Afterwards, in the last stage of the study, lean conditions with 1.5 and 2 air excess ratios thanks to broader flammability limits of hydrogen fuel was investigated in order to control the predicted increase in NO_x emissions caused by the hydrogen use. By taking maximum brake mean effective pressure into consideration, ignition timing should be advanced by increasing air excess ratio of hydrogen fuel due to slower combustion. However, the same ignition timing was chosen for three air excess ratio of hydrogen fuel in order to provide sufficient reduction in NO_x emissions. Moreover, the total measurement uncertainty was obtained using the Kline and McClintock method as shown in Table 3.

Results and discussion

As for the first part of this section, we compared the brake engine torque, brake engine power, brake mean effective pressure, brake thermal efficiency, brake specific fuel consumption, CO, THC and NO_x data obtained by one dimensional model with the use of hydrogen fuel only and gasoline fuel only. Obtained results showed that, the use of hydrogen fuel in the stoichiometry operating conditions resulted in a

Table 3 – Accuracy values of test devices and obtained total uncertainties.

Parameter	Device	Accuracy
Engine speed	Incremental encoder	± 5 rpm
In-cylinder pressure	Kistler 6118B	± 0.3 bar
Gasoline flow rate	Biotech VZS-005	$\pm 1\%$ (of reading)
CO	AVL Digas 4000	0.01% Vol.
THC	AVL Digas 4000	1 ppm
NO_x	AVL Digas 4000	1 ppm
Calculated results		Uncertainty value
Brake thermal efficiency		$\pm 1.18 \div 1.32\%$

dramatic increase in NO_x emissions. Therefore, in the last phase of the work, lean operation conditions with hydrogen fuel (thanks to the wide flammability limits of hydrogen fuel) was investigated by using engine model built in AVL Boost program. Simulations were executed at 3300 rpm constant engine speed, with 1, 1.5 and 2 air excess ratios. Thanks to improved thermal losses due to thicker thermal boundary of leaner hydrogen mixture in addition to high flame speed and wide flammability limits of hydrogen fuel, it was predicted that BTE would increase and engine power and torque reductions would not be significant at extremely lean hydrogen operations in comparison with that of pure gasoline operation.

Engine torque values of gasoline and hydrogen fuel operations with AVL software at different engine speeds are given in Fig. 4. As seen in the figure, the maximum brake engine torque values of gasoline and hydrogen operations occurred at 3100 rpm and 3200 rpm engine speeds, respectively. Additionally, the maximum brake engine torque difference between gasoline and hydrogen fuel resulted in 16.1% at 3100 rpm engine speed. Brake engine torque values were reduced due to the low energy density of the hydrogen fuel in volume, similar to the brake power results.

Fig. 5 shows the results of the brake engine power obtained with the help of the 1-D model as a result of working with gasoline and working with hydrogen fuel at different engine speeds. In the analysis results, it was found that the brake engine power was significantly reduced by working under the stoichiometry condition with hydrogen fuel. The maximum difference in the value of the brake engine power was observed at 3100 rpm engine speed with hydrogen use, a 16.1% decrease was obtained in comparison to the gasoline fuel condition. As a result of the study, the LHV of hydrogen is lower than that of gasoline in volume due to the low density, therefore, engine power was decreased at stoichiometric operation.

The effects of hydrogen fuel use on brake mean effective pressure values at different engine speeds are shown in Fig. 6. Analyses results revealed that BMEP values were decreased by

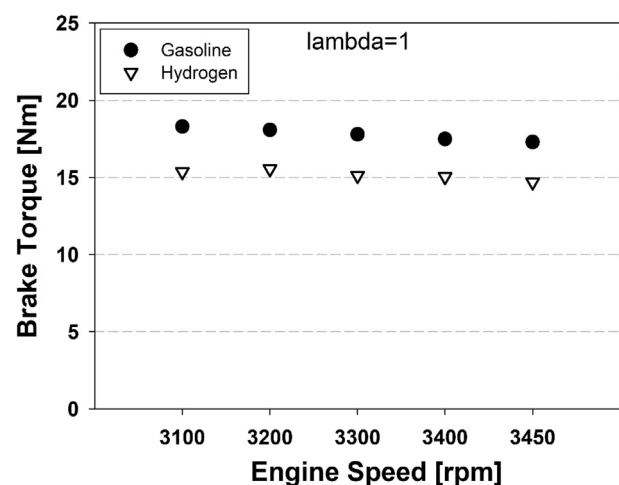


Fig. 4 – Comparison of brake engine torque values at different engine speeds with gasoline and hydrogen fuel at stoichiometry.

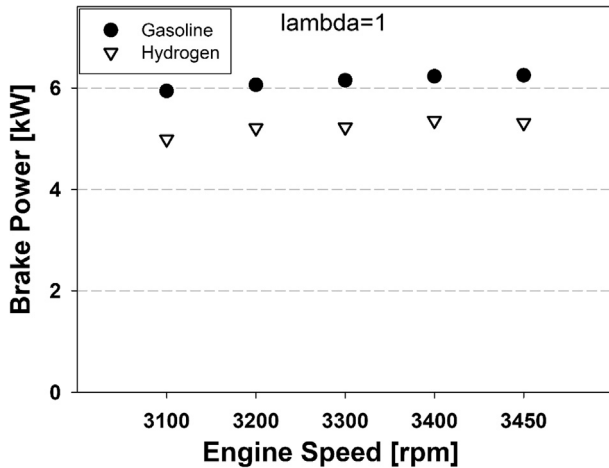


Fig. 5 – Comparison of brake engine power values at different engine speeds with gasoline and hydrogen fuel at stoichiometry.

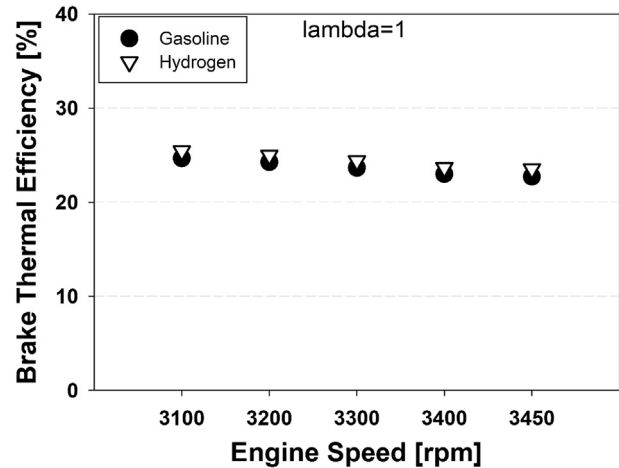


Fig. 7 – Comparison of brake thermal efficiency values at different engine speeds with gasoline and hydrogen fuels at stoichiometry.

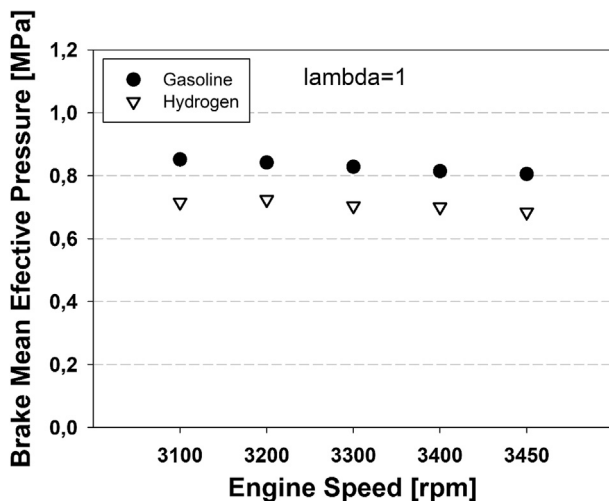


Fig. 6 – Comparison of brake mean effective pressure values at different engine speeds with gasoline and hydrogen fuel at stoichiometry.

using hydrogen as fuel under the stoichiometric condition. Trends of BMEP variations by engine speed and BMEP decrease during hydrogen fuel use show similarities to those of engine power values since BMEP is one of the main parameters of engine power. The maximum reduction of BMEP was 16.1% and it occurred at a 3100 rpm engine speed. Lower energy density of hydrogen in volume caused the decrease in brake mean effective pressure since the same cylinder volume was filled with fuels under stoichiometric conditions ($V_H = 270 \text{ cm}^3$). The same proportional reductions were observed in engine torque, engine power and BMEP (as can be calculated with Eqs. (2) And (3) which were stated in Data Reduction section ($N_e = \frac{2\pi n}{60} M_e$, $BMEP = M_e \frac{4}{V_H n}$) at 3100 rpm engine speed, since these three parameters are directly proportional in the case of the same engine speed ($n = 3100 \text{ rpm}$).

Fig. 7 shows the results of brake thermal efficiency obtained with the one-dimensional model as result of working with gasoline and working with hydrogen at different engine

speeds. The analysis results show that the brake thermal efficiency is significantly improved by hydrogen fuel at full load and under the stoichiometry condition. According to the results, the use of hydrogen fuel resulted in the maximum brake thermal efficiency increase of 3.7% at engine speed of 3450 rpm. The reason for the improvement in the brake thermal efficiency value was that the combustion approaches the ideal constant volume process in the thermodynamic cycle with the help of high flame speed of hydrogen [33], which is resulted in higher maximum pressure and lower loss of work (area) on indicator diagram.

Fig. 8 shows brake-specific fuel consumption values of gasoline and hydrogen fuel operations at different engine speeds. Fuel consumption values of hydrogen operation results were calculated as gasoline equivalent in order to compare different fuels. As seen in Fig. 8 and 328 g/kWh and 318 g/kWh minimum brake-specific fuel consumption values were obtained at 3100 rpm engine speed during gasoline and

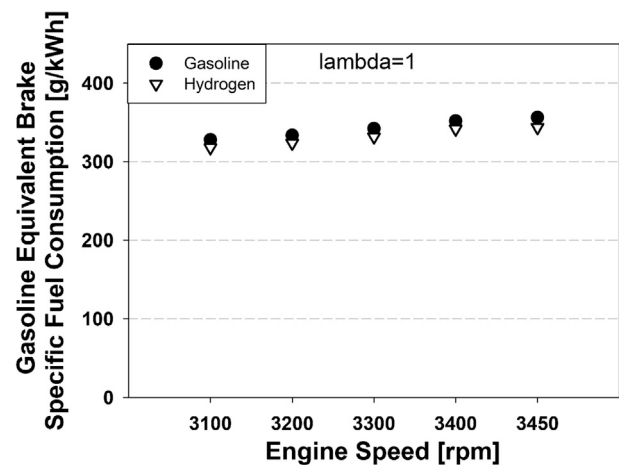


Fig. 8 – Comparison of brake specific fuel consumption values at different engine speeds with gasoline and hydrogen fuels at stoichiometry.

hydrogen fuels operations, respectively. On the other hand, a 3.53% maximum reduction in BSFC occurred by using hydrogen as fuel at 3450 rpm engine speed. The reduction in BSFC was caused by thermal efficiency improvement with the help of rapid combustion of hydrogen, which is more similar to constant volume combustion.

Fig. 9 gives a comparison of the CO emission values, which were only found under gasoline fuel operating conditions, at different engine speeds. CO emission during hydrogen fuel operations were merely noticeable. The results showed that a significant decrease in the brake-specific CO emissions was obtained by the use of hydrogen. As result of hydrogen fuel operations at 3100, 3200, 3300, 3400 and 3450 rpm engine speeds, specific CO emissions were reduced by 11.5, 9.9, 10.9, 9.7 and 8.3 times, respectively, when compared to gasoline fuel operations. This is due to the fact that hydrogen is a fuel that does not contain C atoms; however, the engine model used in this study was built so that some amount of lubricant on the walls would be included in the combustion process. Therefore, CO emissions existed because of the combustion of some lubrication oil in the combustion chamber.

A comparison of the THC emission values, which were revealed under operating conditions with gasoline and conditions with hydrogen fuels at different engine speeds, are presented in Fig. 10. As a result of the executed analysis, specific THC emission values were close to 0 with the use of hydrogen fuel. The THC values obtained using hydrogen were very low due to the lubricating oil. The improvement in brake-specific THC emission values is normal and resulted from the combustion of lubricant as mentioned previously, because the hydrogen is a fuel that does not contain C atoms.

Fig. 11 presents a comparison of NO_x emissions values with gasoline and hydrogen at different engine speeds. From the results obtained, the dramatic increase in NO_x emissions by the hydrogen use cannot be prevented. The maximum increase in NO_x emissions with hydrogen fuel was tested to be 99.5% at engine speed of 3200 rpm. The minimum increase in NO_x emissions was reached at 3300 rpm engine speed by 83.6%. The main reason for the aggressive increase in NO_x

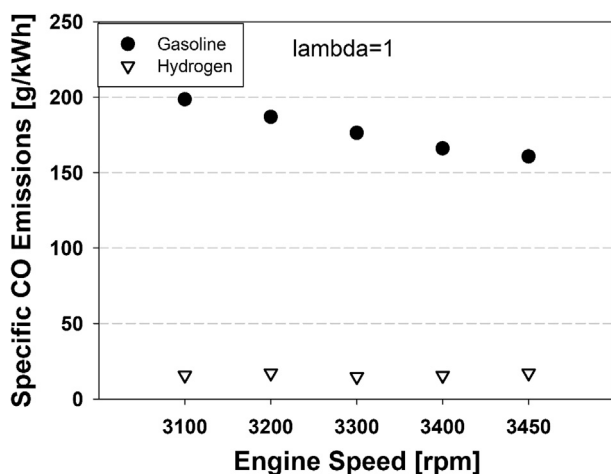


Fig. 9 – Comparison of CO emission values at different engine speeds with gasoline and hydrogen fuels at stoichiometry.

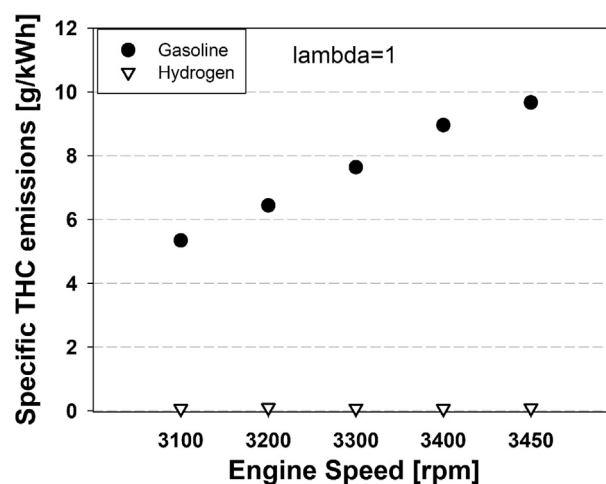


Fig. 10 – Comparison of THC emissions values at different engine speeds with gasoline and hydrogen fuels at stoichiometry.

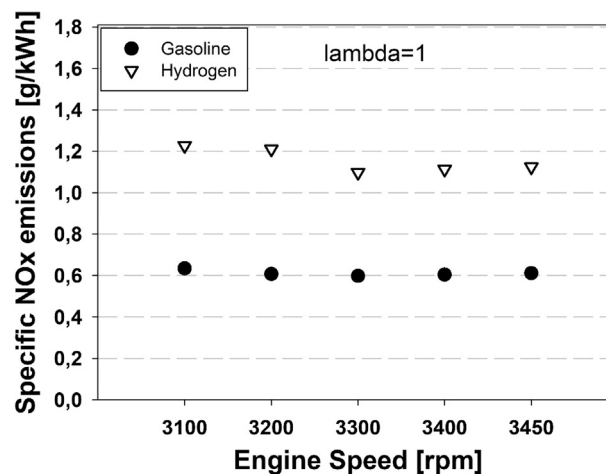


Fig. 11 – Comparison of NO_x emissions values at different engine speeds with gasoline and hydrogen fuels at stoichiometry.

emissions was a result of high peak in-cylinder temperature values due to higher flame speed of hydrogen at stoichiometric conditions than that of gasoline.

Table 4 shows performance and emission parameters values and % differences between gasoline and hydrogen fuel operations at the engine speeds at which the maximum differences were occurred.

Fig. 12 shows the results of operation with gasoline at stoichiometry and hydrogen at different air excess ratios ($\lambda = 1$, $\lambda = 1.5$, $\lambda = 2$). As mentioned before, ignition timing was delayed during hydrogen use in comparison with gasoline operation. But ignition timing was not advanced by increasing air excess ratios in order to suppress NO_x emissions sufficiently. Performance and emission results shown in Fig. 12 are brake engine torque, brake engine power, brake mean effective pressure, brake thermal efficiency, brake specific fuel consumption, brake specific CO emissions, brake specific THC emissions and brake specific NO_x emissions values,

Table 4 – Performance and emission parameters differences between gasoline and hydrogen fuel operations at the engine speeds of the maximum differences were occurred.

Parameters	Engine speed (for the maximum difference) [rpm]	Gasoline fuel results	Hydrogen fuel results	Difference [%]
M_e [Nm]	3100	18.30	15.37	-16.1
N_e [kW]	3100	5.94	4.99	-16.1
BMEP [MPa]	3100	0.85	0.72	-16.1
BTE [%]	3450	23.54	22.71	3.7
BSFC [g/kWh] (Gasoline equivalent)	3450	356	344	-3.53
CO [g/kWh]	3100	198	negligible	-
THC [g/kWh]	3450	9.67	negligible	-
NO_x [g/kWh]	3200	1.211	0.607	99.5

respectively. From the results obtained, it was determined that the brake engine torque and brake engine power value decreased with an increasing excess air ratio value of hydrogen, and the maximum decrease in brake mean effective pressure, brake engine torque and power reached to 44.8%, as seen in Fig. 12. The increased air excess ratio was responsible for the torque and power drops due to a lower amount of hydrogen which can be taken by the cylinder per cycle, in comparison to that of low air excess ratios. To be more precise, when the excess air ratio equals to 1.5 and 2, hydrogen mass values taken into cylinder per cycle reduce by 26.35% and 41.71%, respectively, compared to excess air ratio of 1. The brake mean effective pressure also decreased with increasing excess air ratio for a similar reason as that of brake engine torque and power. On the other hand, there was a slight improvement in brake thermal efficiency with increased excess air ratio by the hydrogen use. With the excess air ratio of 2, the improvement in brake thermal efficiency was up to 4.7% compared to that of gasoline fuel. In this study, the simulations were executed at full load and under stoichiometric conditions, which are better conditions for gasoline combustion in terms of brake thermal efficiency. Hence, it can be predicted that BTE improvement of hydrogen fuel compared to gasoline fuel would be more significant at partial loads [1], since a higher flame speed and completed combustion of hydrogen are less sensitive to in-cylinder temperature decrease and flame out. Increased air excess ratio and oxygen concentration lead hydrogen flame speed to reduce slightly and BTE can be supposed to decrease. However, the peak BTE region of hydrogen fuel is further to the lean mixtures [34]. This can be explained by the fact that during an excess air ratio increase, wide flammability and higher burning velocity of hydrogen keep flame speed reduction at very low levels [5], while lean hydrogen combustion improves thermal losses due to increasing quenching distance and a thicker thermal boundary [22]. These effects lead BTE of hydrogen combustion to improve until further lean mixtures [35,36]. Hence, from 1 to 2 excess air ratios, brake thermal efficiency was slightly improved. As shown in Fig. 12, gasoline equivalent brake specific fuel consumption trend occurred as opposed to the BTE trend. The use of hydrogen with 2 excess air ratio was provided by a 4.7% maximum improvement in BSFC at 3300 rpm engine speed. On the other hand, no significant improvement in CO emissions was observed with the hydrogen operations in the different air excess coefficients. Specific CO emissions, which were

obtained during excess air ratio of 1, 1.5 and 2 operations, were reduced by 10.9, 11.2 and 11.1 times, respectively, compared to gasoline fuel operations. The reason for this is that CO comes from burning the lubricating oil, which was released due to the presence of C atoms. Likewise, no significant change in THC emissions was observed by the change in the air excess coefficient. However, notable improvements occurred in NO_x emissions due to the air excess coefficient. The biggest reason for this is the combustion of hydrogen under extremely lean conditions with an increased air excess coefficient. Thus, NO_x emissions can be controlled by reducing the in-cylinder peak temperatures by increasing air excess ratio. The use of hydrogen increased NO_x emissions by 83.6% under stoichiometry. However, when the value of the excess air ratio was increased to 1.5, it was only a 20.1% increase in specific NO_x emissions compared to the gasoline condition. As a result of the air excess ratio reaching 2, specific NO_x emissions decreased by 1.1%, which means improvement in NO_x emissions compared to the condition of using gasoline only. Briefly, 1.1% decrease in NO_x and 4.7% increase in BSFC were obtained by increasing air excess ratio up to 2, while engine power reduction was 44.8% compared to gasoline operation. The mentioned decrease in engine power is acceptable and still useful especially in hybrid systems with low-powered engines since BSFC and NO_x were improved.

Fig. 13 shows the variations of in-cylinder pressure, normalized heat-release rate, in-cylinder temperature and P-V diagram under stoichiometry with pure gasoline, at stoichiometry and lean conditions with hydrogen. As can be seen in Fig. 13.a, the ignition timing was delayed 3.5° CA with the hydrogen fuel operation by taking higher flame speed of hydrogen into consideration in order to obtain maximum brake mean effective pressure. According to the results, it was found that even though there was a lower hydrogen energy content in cylinder per cycle compared to gasoline, peak pressure values of hydrogen fuel operation were higher than that of gasoline operation at $\lambda = 1$ and $\lambda = 1.5$ due to a wide flammability range and high flame speed of hydrogen. However, when λ reaches 2, the peak pressure value of hydrogen operation drops below the gasoline peak pressure at 3300 rpm engine speed. Accordingly, a similar trend occurred for in-cylinder temperature values, which led NO_x emissions in the hydrogen operation to drop below NO_x emissions in the gasoline operation under $\lambda = 2$ condition [37]. Likewise, the normalized heat release rate values also decrease with increasing air excess ratio. This is due to the increase of the air excess ratio and the decrease of the

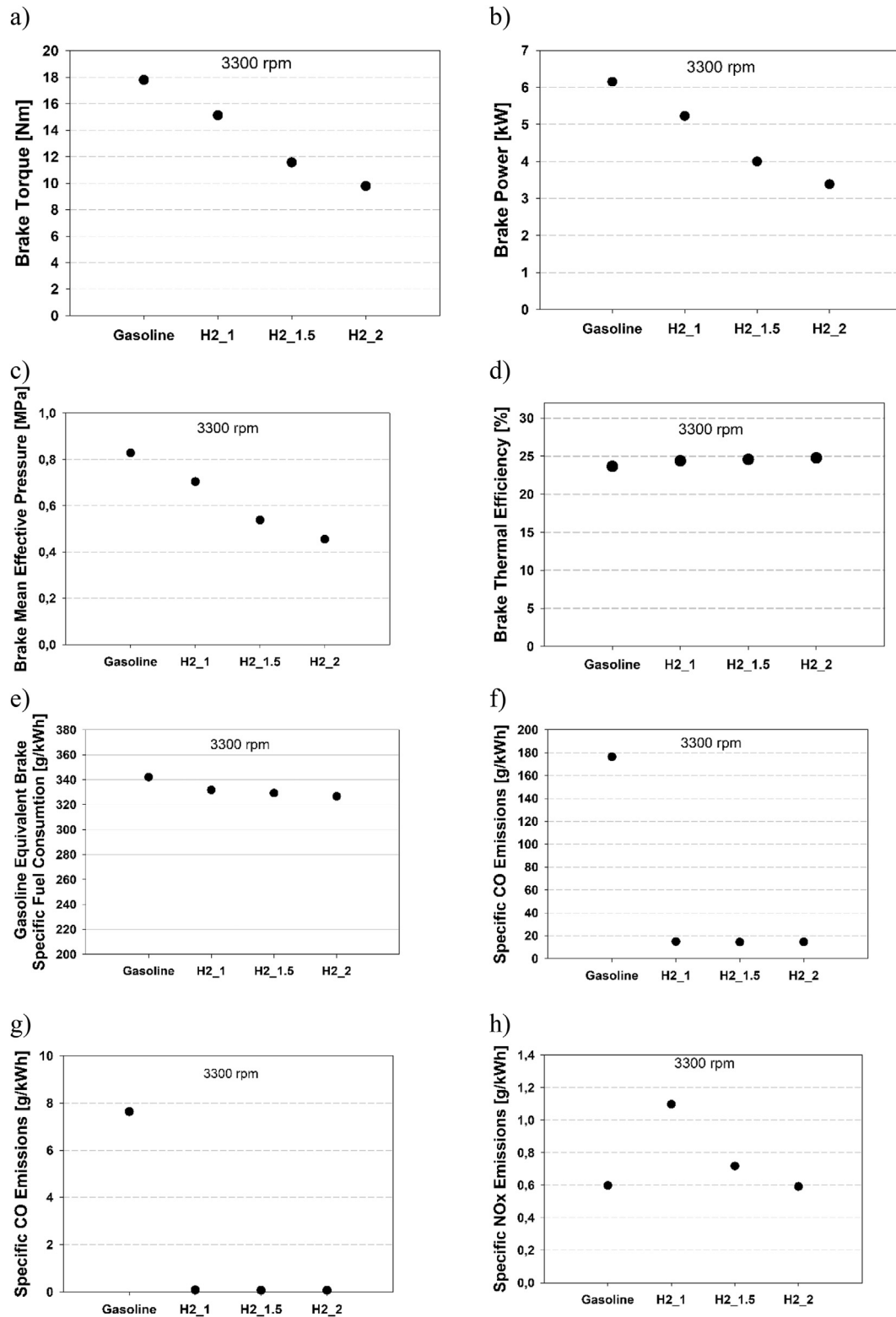


Fig. 12 – a) Brake torque values, b) Brake power values, c) Brake mean effective pressure d) Brake thermal efficiency values, e) Brake specific fuel consumption (gasoline equivalent) f) Brake specific CO emission values, g) Brake specific THC emission values and h) Brake specific NO_x emission values with gasoline at stoichiometry and hydrogen at different excess air ratios.

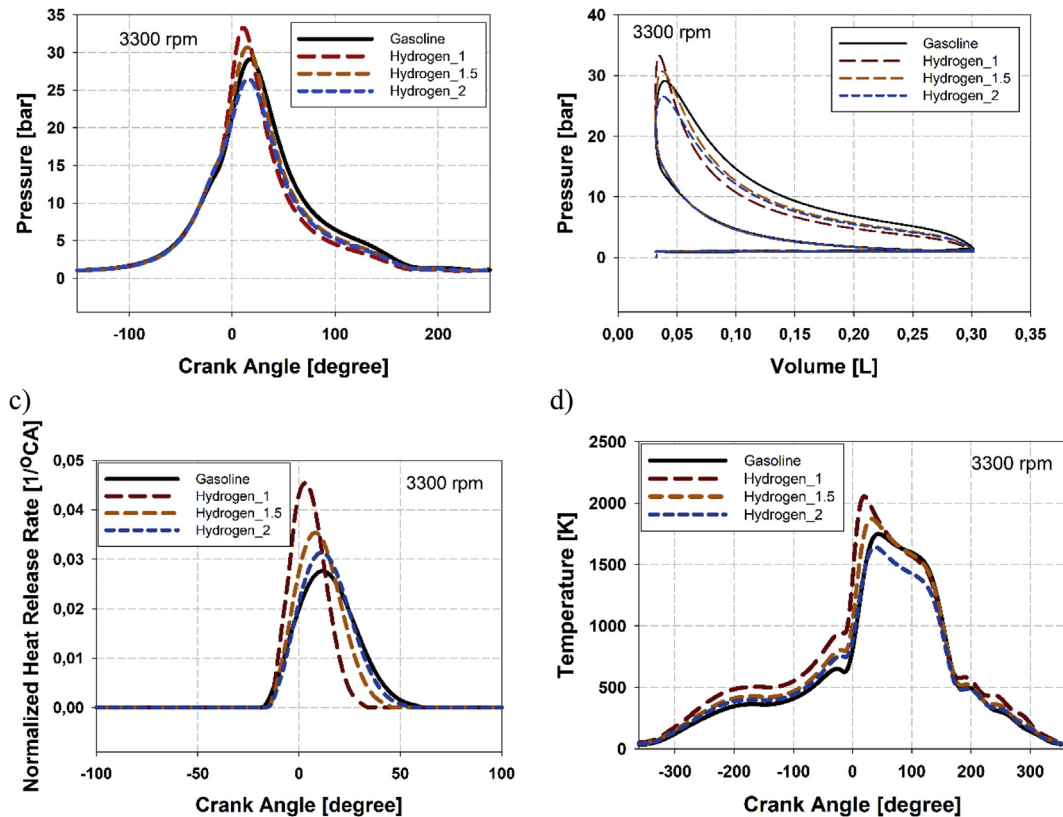


Fig. 13 – a) In-cylinder pressure data, b) Indicator diagram, c) Normalized heat release rate values, and d) In-cylinder temperature values with gasoline at stoichiometry and hydrogen at different excess air ratios.

energy value introduced into the cylinder per unit cycle and the decrease of the combustion speed. Also, using hydrogen, the combustion period approaches an ideal constant volume heat input process owing to unique properties of hydrogen, as can be seen in the P–V diagram.

Conclusion

In the study conducted, the theoretical model, which was developed by using AVL Boost software, was validated with the experimental results in the first stage with gasoline fuel at stoichiometry. Then, results obtained through the analyses of pure hydrogen fuel and pure gasoline fuel operations under stoichiometric condition, full load and different engine speeds (3100 rpm, 3200 rpm, 3300 rpm, 3400 rpm and 3450 rpm) were compared. Since the dramatic increase in NO_x emissions couldn't be avoided, the air excess ratio of hydrogen fuel was changed, and the analysis was performed up to 2 air excess ratios at a constant engine speed of 3300 rpm by means of wide flammability limits and higher flame speed of hydrogen. Afterwards, these latest results were also compared with those of a baseline fuel of gasoline. Concluding remarks of the present study are as follows:

- An acceptable difference between pressure and normalized heat release rate values of experimental and theoretical results were obtained with gasoline fuel. The other performance and emission results were also adequately

overlapped, with the exception of THC. Apart from THC emissions, the maximum error rate was 4.5% and was observed at CO emission value.

- The simulation results showed that the use of hydrogen fuel improved brake thermal efficiency at different engine speeds even though the brake power value has decreased. Emissions of CO and THC were close to zero; however, a dramatic increase of up to 99.5% of NO_x emissions were not prevented.
- At the last stage of the study, dramatic increase in NO_x emissions was eventually suppressed by using extremely lean ($\lambda = 2$) hydrogen operation. Although the air excess coefficient reached 2, the brake thermal efficiency value obtained was higher than that of gasoline.
- At 3300 rpm constant engine speed and the extremely lean operation conditions with hydrogen fuel, 1.1% and 4.7% improvements were obtained in NO_x and BSFC, respectively, while 44.8% reduction was obtained in engine power compared to gasoline operation. However, it was concluded that this extremely lean hydrogen fueled engine is useful for hybrid systems as a clean (negligible CO and THC, lower NO_x in compared to that of gasoline) power source, since some hybrid systems require low-powered ICEs.

Acknowledgements

This research was supported by TUBITAK (Scientific and Technological Research Council of Turkey) with 1512 project. Project Number: 2150175. The authors are also indebted to

Şahin Metal A.Ş. and Erin Motor for providing us with test apparatus and equipment donation. The second author of the manuscript has been financially supported by TUBITAK 2228-B program.

Nomenclature

BMEP	Brake mean effective pressure
BSFC	Brake specific fuel consumption
BTE	Brake Thermal Efficiency
BTDC/ATDC	Before/After top death center
CA	Crank angle
CI	Compression ignition
CNG	Compressed natural gas
CO	Carbon monoxide
CO ₂	Carbon dioxide
DC/AC	Direct current/Alternative current
EGR	Exhaust gas recirculation
FC	Fuel Cell
HC	Hydrocarbons
HRR	Heat Release Rate
ICEs	Internal combustion engines
LHV	Lower heating value
NO _x	Oxides of nitrogen
PEMFC	Proton Exchange Membrane Fuel Cell
RPM	Repeat per minute
SI	Spark ignition
TDC/BDC	Top/Bottom Death Center
THC	Total unburned hydrocarbons

REFERENCES

- [1] Sims R, Schaeffer R, Creutzig F, Cruz-Núñez X, D'Agosto M, Dimitriu D, Figueroa Meza MJ, Fulton L, Kobayashi S, Lah O, McKinnon A, Newman P, Ouyang M, Schauer JJ, Sperling D, Tiwari G. Transport. In: Edenhofer O, Pichs-Madruga R, Sokona Y, Farahani E, Kadner S, Seyboth K, Adler A, Baum I, Brunner S, Eickemeier P, Kriemann B, Savolainen J, Schlömer S, von Stechow C, Zwickel T, Minx JC, editors. Climate change 2014: mitigation of climate change. Contribution of working group III to the fifth assessment report of the intergovernmental panel on climate change. Cambridge, United Kingdom and New York, NY, USA: Cambridge University Press; 2014.
- [2] European Environment Agency. Electric vehicles in Europe. Copenhagen: EEA; 2016. Report No 20/2016.
- [3] Zighmi S, Mennouche D, Goudjil MB, Ladjel S, Ayachi AO. Experimental exploitation of solar energy for drying peanut from Algeria and production of renewable biofuel. The 6th European Conference on Renewable energy systems (ECRES 2018) Istanbul/Turkey 25-27 June. 2018. p. 285–93.
- [4] Köten H, Balci Ö, Karagöz Y. Effect of different levels of ethanol addition on performance, emission and combustion characteristics of A gasoline engine. The 6th European Conference on Renewable energy systems (ECRES 2018) Istanbul/Turkey 25-27 June. 2018. p. 674–85.
- [5] Ji CW, Wang SF. Effect of hydrogen addition on combustion and emissions performance of a spark ignition gasoline engine at lean conditions. *Int J Hydrogen Energy* 2009;34:7823–34. <https://doi.org/10.1016/j.ijhydene.2009.06.082>.
- [6] Ji CW, Wang SF. Effect of hydrogen addition on the idle performance of a spark ignited gasoline engine at stoichiometric condition. *Int J Hydrogen Energy* 2009;34:3546–56. <https://doi.org/10.1016/j.ijhydene.2009.02.052>.
- [7] Heffel JW. NO_x emission reduction in a hydrogen fueled internal combustion engine at 3000 rpm using exhaust gas recirculation. *Int J Hydrogen Energy* 2003;28:1285–92. [https://doi.org/10.1016/S0360-3199\(02\)00289-6](https://doi.org/10.1016/S0360-3199(02)00289-6).
- [8] Dhyani V, Subramanian KA. Experimental investigation on effects of knocking on backfire and its control in a hydrogen fueled spark ignition engine. *Int J Hydrogen Energy* 2018;43(14):7169–78. <https://doi.org/10.1016/j.ijhydene.2018.02.125>.
- [9] Li H, Karim GA. Knock in spark ignition hydrogen engines. *Int J Hydrogen Energy* 2004;29:859–65. <https://doi.org/10.1016/j.ijhydene.2003.09.013>.
- [10] Verhelst S, Maesschalck P, Rombaut N, Sierens R. Efficiency comparison between hydrogen and gasoline, on a bi-fuel hydrogen/gasoline engine. *Int J Hydrogen Energy* 2009;34(5):2504–10.
- [11] Kosmadakis GM, Rakopoulos CD, Demuynck J, De Paepe M, Verhelst S. CFD modeling and experimental study of combustion and nitric oxide emissions in hydrogen-fueled spark-ignition engine operating in a very wide range of EGR rates. *Int J Hydrogen Energy* 2012;37(14):10917–34.
- [12] Nieminen J, Dincer I. Comparative exergy analyses of gasoline and hydrogen fuelled ICEs. *Int J Hydrogen Energy* 2010;3(5):5124–32. <https://doi.org/10.1016/j.ijhydene.2009.09.003>.
- [13] Lucas G, Richards W. The hydrogen/petrol engine - the means to give good part-load thermal efficiency. SAE Technical Paper 820315, <https://doi.org/10.4271/820315>; 1982.
- [14] Ji C, Wang S, Zhang B, Liu X. Emissions performance of a hybrid hydrogen–gasoline engine powered passenger car under the New European Driving Cycle. *Fuel* 2013;106:873–5.
- [15] Huang Z, Zhang Y, Zeng K, Liu B, Wang Q, Jiang D. Measurements of laminar burning velocities for natural gas-hydrogen-air mixtures. *Combust Flame* 2006;146(1–2):302–11.
- [16] Erjiang Hu E, Huang Zuohua, He Jiajia, Jin Chun, Zheng Jianjun. Experimental and numerical study on laminar burning characteristics of premixed methane-hydrogen-air flames. *Int J Hydrogen Energy* 2009;34(11):4876–88.
- [17] Huang Zuohua, Liu Bing, Zeng Ke, Huang Yinyu, Jiang Deming, Wang Xibin, Miao Haiyan. Combustion characteristics and heat release analysis of a spark-ignited engine fueled with natural gas-hydrogen blends. *Energy Fuel* 2007;21(5):2594–9.
- [18] Huang Zuohua, Liu Bing, Zeng Ke, Huang Yinyu, Jiang Deming, Wang Xibin, Miao Haiyan. Experimental study on engine performance and emissions for an engine fueled with natural gas-hydrogen mixtures. *Energy Fuel* 2006;20(5):2131–6.
- [19] Hu Erjiang, Huang Zuohua, Liu Bing, Zheng Jianjun, Gu Xiaolei, Huang Bin. Experimental investigation on performance and emissions of a spark-ignition engine fuelled with natural gas-hydrogen blends combined with EGR. *Int J Hydrogen Energy* 2009;34(1):528–39.
- [20] Hu Erjiang, Huang Zuohua, Liu Bing, Zheng Jianjun, Gu Xiaolei. Experimental study on combustion characteristics of a spark-ignition engine fuelled with natural gas-hydrogen blends combining with EGR. *Int J Hydrogen Energy* 2009;34(2):1035–44.
- [21] Ceviz MA, Sen AK, Küleri AK, Öner İV. Engine performance, exhaust emissions, and cyclic variations in a lean-burn SI

- engine fueled by gasoline hydrogen blends. *Appl Therm Eng* 2012;36:314–24.
- [22] Schefer RW, White C, Keller J. Lean hydrogen combustion. Academic Press. Technology and Control; 2008. p. 213–54 [Chapter 8], <https://doi.org/10.1016/B978-012370619-5.50009-1>.
- [23] Wang S, Ji C, Zhang B, Liu X. Lean burn performance of a hydrogen-blended gasoline engine at the wide open throttle condition. *Appl Energy* 2014;136:43–50. <https://doi.org/10.1016/j.apenergy.2014.09.042>.
- [24] Niu R, Yu X, Du Y, Xie H, Wu H, Sun Y. Effect of hydrogen proportion on lean burn performance of a dual fuel SI engine using hydrogen direct-injection. *Fuel* 2016;186:792–9.
- [25] Heywood JB. Internal combustion engine fundamental. New York: McGraw-Hill, Inc.; 1988.
- [26] Karagöz Y, Sandalcı T, Dalkılıç AS. Effects of hydrogen and oxygen enrichment on performance and emissions of an SI engine under idle operating condition. *Int J Hydrogen Energy* 2015;40(28):8607–19. <https://doi.org/10.1016/j.ijhydene.2015.05.006>.
- [27] Singh P, Chauhan SR, Goel V. Assessment of diesel engine combustion, performance and emission characteristics fuelled with dual fuel blends. *Renew Energy* 2018;125:501–10.
- [28] Kolchin A, Demidov V. Design of automotive engines. Moscow: MIR Publishers; 1984.
- [29] Rolf E. Combustion diagnostics by means of multizone heat release analysis and no calculation. SAE Tech Pap Ser 1998;107.
- [30] AVL LIST GmbH Hans-List-Platz 1. A-8020 graz. Edition 11. 2013. Austria, BOOST v2013.2.
- [31] VDMA Engines and Systems. Exhaust emission legislation diesel- and gas engines. Frankfurt: VDMA; 2017.
- [32] Kline SJ, McClintock FA. Describing uncertainties in single-sample experiments. *Mech Eng* 1953;75:3–8.
- [33] Shivaprasad KV, Raviteja S, Chitragar Parashuram, Kumar GN. Experimental investigation of the effect of hydrogen addition on combustion performance and emissions characteristics of a spark ignition high speed gasoline engine. *Procedia Tech* 2014;14:141–8.
- [34] Kornbluth K, Greenwood J, McCaffrey Z, Vernon D, Erickson P. Extension of the lean limit through hydrogen enrichment of a LFG-fueled spark-ignition engine and emissions reduction. *Int J Hydrogen Energy* 2010;35(3):1412–9.
- [35] Luo Q, Sun B. Experiments on the effect of engine speed, load, equivalence ratio, spark timing and coolant temperature on the energy balance of a turbocharged hydrogen engine. *Energy Convers Manag* 2018;162:1–12.
- [36] Negurescu N, Pana C, Cernat A. Aspects of using hydrogen in SI engine. *U.P.B. Sci Bull Series D* 2012;74(1):1454–2358.
- [37] Egnell R. Combustion diagnostics by means of multizone heat release analysis and NO calculation, SAE international spring fuels and lubricants meeting and exposition dearborn, Michigan, 4-6 May. 1998.